Study on Heat Transfer and Flow Resistance Characteristics of Typical Heat Exchanger Tube Based on Adaptive Heat Transfer Enhancement Method

Yongxiang Ren[1(✉)], Xiao Yu[2], and Bensi Dong[2]

[1] AECC Shenyang Engine Research Institute, Shenyang, China
[2] Beijing University of Aeronautics and Astronautics, Beijing, China

Abstract. Aiming at improving heat transfer efficiency of heat exchanger tube, this paper proposes two types of tape fitted in tubes with adaptive transform capabilities(different twisted ratio and shrink ratio at different temperature) and study on the heat transfer and flow characteristics inside the tube. In this study, the performance of inserts is simulated by commercial computational fluid dynamics (CFD) solver. Two types of inserts are presented as twisted tape and ripple tape. To value the performance of the tapes, the results simulated by CFD are presented in dimensionless form such as Nusselt number(Nu), friction factor(f) and performance evaluation criteria (PEC). Meanwhile, through the results, several dimensionless correlations are developed to predict the heat transfer characteristics and flow resistance of the heat exchanger tube with different types of tape.

Keywords: Twisted tape · Ripple tape · Enhanced heat transfer

1 Introduction

As the demand of high thrust-weight ratio of aircraft engine increases more and more, the heat load inside the engine is also becoming heavier. Therefore heat transfer for a better temperature distribution inside the engine is necessary. As the most important component for the heat transfer, heat exchangers are used heavily. The efficiency of the heat ex-changer is the key to value the performance. In recent years, Many researchers have been studying on heat transfer enhancement measures [1–10].

Heat transfer enhancement measures can be divided into two parts: active heat transfer enhancement and passive heat transfer enhancement. Active heat transfer enhancement requires outside power such as vibration or else to change the flow field and to enhance the heat transfer. However, the passive heat transfer enhancement does not require outside power to create the high intensity flow to improve heat transfer. Base on this feature, passive heat transfer enhancement measures are applied in a large amount of engineering practices. Many researchers have studied on the mechanism of passive heat transfer. Zimparov et al. [11–14] studied the flow and heat transfer characteristics of spiral grooved tube com-bined with twisted tape experimentally, and summarized

the flow and heat transfer correlations. Bas et al. [15]. studied heat transfer and flow characteristics of tubes fitted with twisted tapes by experiments. It is found that the heat transfer intensity is affected by the twisted ratio of the tape, the intensity of heat transfer is improving when the twisted ration decreases. Savekar, Arsha, Salman et al. [16–18]. studied on the relationship between Nusselt number, Reynolds number and twisted ratio. The study found that Nusselt number increases when the Reynolds number increases. Hossain el at. [19] found that compared to the tube without obstacle, the heat transfer capacity of the tube with obstacles inside it is larger. The distance between obstacles has a crucial effect on heat transfer. Meng et al. [20]. found that the heat transfer intensity in discrete double-inclined ribs tube is much higher than the normal tube. Nusselt number inside the tube is 250%–650% of the tube without discrete double-inclined ribs and the flow resistance is 120%–300% simultaneously. The study of Bhuiya et al. [21]. shown that by inserting two-reverse-direction twisted tape, the Nusselt number, friction and PEC in-crease when the twisted ratio decreases. When Reynolds number is low and the twisted ratio reaches to 1.95, the maxi-mum PEC is acquired. Zhang et al. [22]. studied on the heat transfer intensity of tube with different types of inserts. It is found that compared to the plain tube, the tube with triple and quadruple tape has a higher heat transfer intensity. Mahfouz et al. [23].study on the heat transfer inside tube with different types of inserts and fitting the formula of Nusselt number, Reynolds number and twisted ratio.

Through the study of the above researchers, it can simply come to a conclusion that fit different types of obstacles can improve heat transfer intensity inside a heat exchanger tube. This paper is aiming at analysis the heat transfer mechanism in a tube with different kinds of inserts and to find out the relationship between Nusselt number, Reynolds number and geometry of the obstacle.

2   Model and Calculation Configuration

To analysis the effect on the heat transfer and resistance characteristics of different inserts, two types of inserts (twisted tape and ripple tape) are studied. The geometry of the twisted tape is showed in Fig. 1. Thickness of tape (δ) is 0.8mm. The screw pitch (L) and diameter of tape(D) are used to describe the twisted ratio($\varepsilon = $ L/D). Geometry of the ripple tape is showed in Fig. 2. Thickness of the ripple tape is δ, ripple tape conforms to sinusoidal law, the shrink ratio (θ) is de-scribe by k and A (θ = k/A).
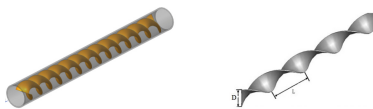

Fig. 1. Geometry of twisted tape   **Fig. 2.** Geometry of ripple tape

The effect of twisted tape and ripple tape on the heat transfer and flow resistance characteristics was studied. To analysis the specific characteristics inside the tube, the commercial computational fluid dynamics software (Ansys Fluent19) was used to solve the governing equation (conservation of mass, momentum, energy and turbulence equations). SIMPLE algorithm was applied to resolve the coupling between velocity and pressure fields with second-order accurate scheme. The working fluid was Air and the flow

was assumed to be steady-state, incompressible and turbulent. Base on the assumption mentioned above, the conservation equation can be described as follow:

$$\frac{\partial u_j}{\partial x_j} = 0 \tag{1}$$

$$\frac{\partial (\rho u_j u_i)}{\partial x_j} = -\frac{\partial p}{\partial x_i} + \frac{\partial}{\partial x_j}[(\mu + \mu_t)\frac{\partial u_i}{\partial x_j} \tag{2}$$

$$\frac{\partial (\rho u_j T)}{\partial x_j} = \frac{\partial p}{\partial x_j}[(\frac{\mu}{P_r} + \frac{\mu_t}{\sigma_T})\frac{\partial T}{\partial x_j} \tag{3}$$

$$\frac{\partial (\rho u_j k)}{\partial x_j} = \frac{\partial}{\partial x_j}[(\mu + \frac{\mu_t}{\sigma_k})\frac{\partial k}{\partial x_j}] + G_k - \beta_1 k\omega \tag{4}$$

$$\frac{\partial (\rho u_j \omega)}{\partial x_j} = \frac{\partial}{\partial x_j}[(\mu + \frac{\mu_t}{\sigma_\omega})\frac{\partial k}{\partial x_j}] + G_\omega - \beta_2 \omega^2 + 2(1 - F_1)\frac{\sigma_{\omega,2}}{\omega}\frac{\partial k}{\partial x_j}\frac{\partial \omega}{\partial x_j} \tag{5}$$

Where u is the flow velocity, ρ is the density of the fluid, x_i, x_j are the Cartesian coordinates, μ is the fluid dynamic viscosity, $\mu\tau$ is the turbulent viscosity, P_r is the Prandtl number, T is the fluid temperature, σ_τ is the turbulent Prandtl number for the temperature, k is the turbulent kinetic energy, Gk is the generation of turbulent kinetic energy, ω is the turbulent specific dissipation rate, G_w is the generation of specific dissipation rate. F_1 is the blending function. σ_k and σ_ω are the turbulent Prandtl numbers for k and ω respectively. β_1, β_2, $\sigma_{\omega,2}$ are model constants. The Geometry of calculation model is shown in Fig. 3. The CFD model specifications and boundary conditions are shown in Table 1.
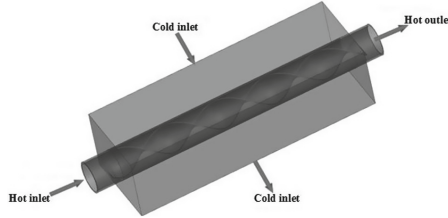

Fig. 3. Geometry of accuracy validation model

3   Grid Independence and Mode Validation

The quantity and quality of grid will have great influence on the calculation results. A grid independence test is performed to minimum the effect on the accuracy of simulation results. The relationship between Nu and the number of grid is shown in Fig. 4 and the relationship between f and the number of grid is shown in Fig. 5, It shows that the correlation between calculated results and number of grid is no longer obvious as the grid number increasing up to 3 × 106.

Table 1. CFD model specifications and boundary conditions.

Geometry/boundary condition	Specification	Value
Tube	Inner diameter	10 mm
	Outer diameter	12 mm
	Length	100 mm
Twisted tape	Twisted ratio (ε)	1, 1.5, 2, 4, 6, 9
Ripple tape	Shrink ratio (θ)	3.33, 4.67, 6.67, 10
Turbulent model	$SST\ k - \omega$	%5 Turbulent intensity
Velocity boundary	Hot inlet (m/s)	5, 10, 15, 20, 25, 30, 35
	Cold inlet (m/s)	5
Temperature boundary	Hot inlet	473 K
	Cold inlet	300 K
Pressure boundary	Hot outlet	101325 Pa
	Cold outlet	101325 Pa
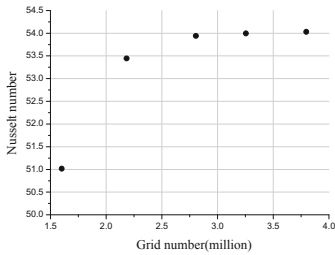
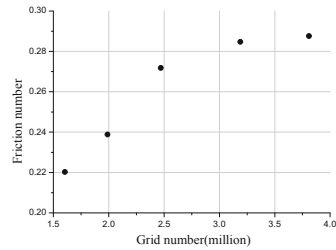**Fig. 4.** Relationship between Nu and grid number

Fig. 5. Relationship between f and grid number

Some researchers have studied about the turbulence models previously to testify the accuracy of this kind of flow. It was shown that the $SSTk - \omega$ turbulence model is in good agreement with the experimental data. A simulation was performed to verify the calculation model accuracy compared to the experimental work from Eiamsa-ard et al. [24]. The result of the simulation was shown in Fig. 6 and Fig. 7. It can be seen from the diagram that the result of Nusselt number is in good agreement with the experimental data where the Reynolds number between 0–12000. The calculated result gradually deviates from the test value as the Reynolds number increasing. It shows that the maximum error of the Nusselt number below 5% when the Reynolds number between 0 to 12000 and the error of friction factor(f) not more than 10%. Considered of the uncertainty of the experimental data (10% of the Nu, 12% of the f). The definition of Nu, Re and f are

given as follow:

$$Nu = \frac{hD}{\lambda} \qquad (6)$$

$$Re = \frac{\rho vD}{\mu} \qquad (7)$$

$$f = \frac{2\Delta pD}{L\rho v^2} \qquad (8)$$

$$Q = Ah(T_{surf} - (\frac{T_{out} + T_{in}}{2})) \qquad (9)$$

Where Q is the heat transfer capacity, Tin, Tout are the fluid temperature of the inlet and outlet. A is the heat transfer area, h is the heat transfer coefficient, ΔP is the pressure difference between inlet and outlet, λ is the thermal conductivity of fluid, v is the fluid velocity.
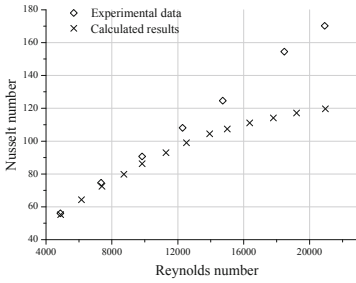
Fig. 6. Comparison of Nu between calculated results and experimental data
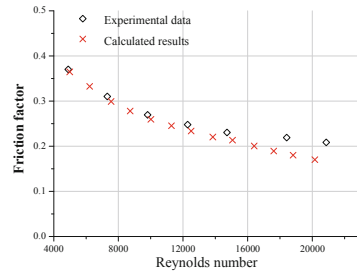

Fig. 7. Comparison of Friction factor between calculated results and experimental data

4   Results and Analysis

4.1   Effects of Twisted Tape on Heat Transfer and Flow Characteristics

The relationship between Nusselt number and Reynolds number at different twisted ratio are given in Fig. 8. It can be seen that the heat transfer intensity increases when the Reynolds number increases. At the same twisted ratio, the Nusselt number with small twisted ratio is higher than which with big twisted ratio.

To find out the specific effect of twisted ration on heat transfer, ΔNu_σ is given to describe the increment of Nusselt number at unit twisted ratio drop. The definition of ΔNu_σ is presented below. $Nu(\varepsilon i, Re_j)$ represent the Nusselt number when the ε is i and the Re is j. Figure 9 shows that as the twisted ratio decreases, the ΔNu_σ increases correspondingly. This suggests that the growth of Nusselt number is not linear with the decrease of twisted ration. When the twisted ration is large, the growth of Nusselt number
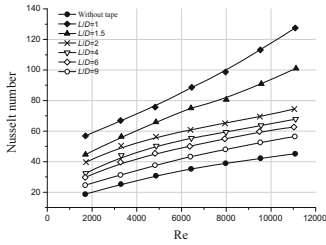
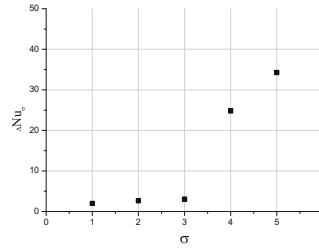**Fig. 8.** Relationship between Nu and Re at different twisted ratio

Fig. 9. Changes in growth of ΔNu_σ

caused by decrease of twisted is not obvious. As the twisted ratio decrease gradually, the heat transfer benefits of the decreasing twisted ratio becoming more and more apparent. When the twisted ratio decreasing from 1.5 to 1, the unit Nusselt number increment is 171% of the Nusselt number as the twisted ratio decreasing from 9 to 6.

$$\Delta Nu_\sigma = \frac{Nu(\varepsilon_\sigma, \overline{Re}) - Nu(\varepsilon_{\sigma-1}, \overline{Re})}{\varepsilon_\sigma - \varepsilon_{\sigma-1}} \tag{10}$$
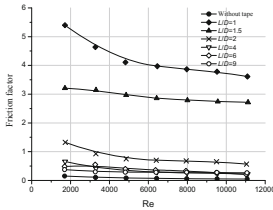

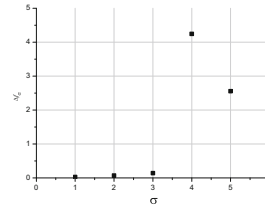**Fig. 10.** Relationship between f and Re at different twisted ratio

Fig. 11. Changes in growth of Δf_σ

The effect of twisted tape is shown in Fig. 10, compared to the tube without twisted tape, flow resistance in the tube with twisted tape is much higher and the friction factor increases as the twisted ratio decreases. At the same twisted ratio, the flow resistance decreases when the Reynolds number increases. That is because as the Reynolds number increasing, the viscous boundary layer is getting thinner, so the drag from the surface is smaller. This phenomenon is much more obvious when the Reynolds number between 2000– 6000. To find out the specific effect of the twisted tape on resistance, Δf_σ is defined to described the unit flow resistance increment as follow:

$$\Delta f_\sigma = \frac{f(\varepsilon_\sigma, \overline{Re}) - f(\varepsilon_{\sigma-1}, \overline{Re})}{\varepsilon_\sigma - \varepsilon_{\sigma-1}} \tag{11}$$

Figure 11 shows that the rate of flow resistance increment is variable, as the twisted ratio decreasing, the flow resistance becoming higher and higher. However, the unit flow resistance increment reaches maximum when the twisted ratio near 1.5, as the twisted

ratio continue goes up, the unit flow resistance increment becomes lower, that means the rate of flow resistance increment declined.

Based on the CFD results shown in Fig. 10, and Fig. 12, two dimensionless correlations (Eqs. 17 and Eqs. 18) for estimating the heat transfer and pressure drop in tubes with twisted tape were developed. The Eqs. 17 relates the Nusselt number to the twisted ratio and Reynolds number while the Eqs.18 relates the Friction factor to the twisted ratio and Reynolds number.

$$Nu = 1.62\varepsilon^{-0.34}Re^{0.45} \tag{12}$$

$$f = 26.9\varepsilon^{-1.61}Re^{-0.21} \tag{13}$$

4.2   Effects of Ripple Tape on Heat Transfer and Flow Characteristics

In this section, the effect of ripple tape on heat transfer and flow characteristics is discussed, It is found that the ripple tape have the ability to improve heat transfer intensity to some degree, with different shrink ratio, the heat transfer enhancement is different. Figure 12 shows the velocity distribution of fluid with different shrink ratio. As the existence of the ripple tape, many acceleration channel are formed at the peak of the tape, this kind of acceleration channel increases the velocity of fluid and the intensity of heat transfer. The larger the shrink ratio is, the more acceleration channels formed, that illustrates how shrink ratio affects the heat transfer intensity.

Figure 13 shows the relationship between the Nusselt number and Reynolds number at different shrink ratio, it can be seen that at the same Reynolds number, the Nusselt number increases as the shrink ratio increases. Figure 14 shows that the ripple tape can also increase the flow resistance despite the heat transfer enhancement.
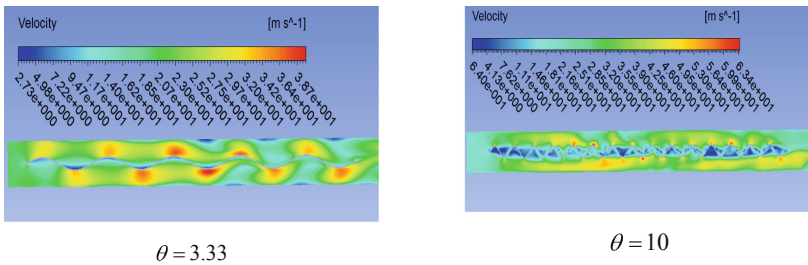

$\theta = 3.33$ $\theta = 10$

Fig. 12. Velocity distribution of fluid with different shrink ratio

Similar to the twisted tape, two dimensionless correlations (Eqs. 19 and Eqs. 20) for estimating the heat transfer and pressure drop in tubes with ripple tape are developed as follow:

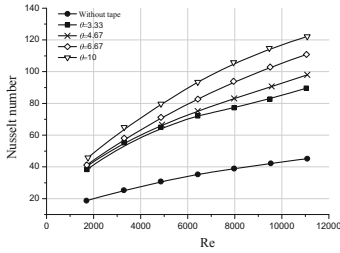$$Nu = 1.62\varepsilon^{-0.34}Re^{0.45} \tag{14}$$

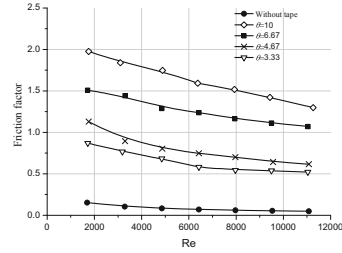**Fig. 13.** Relationship between Nu and Re at different shrink ratio

Fig. 14. Relationship between f and Re at different shrink ratio

$$f = 26.9\varepsilon^{-1.61}Re^{-0.21} \tag{15}$$

In order to find out how to fulfill the most benefits according to inserts, PEC is presented to value the performance of the tape combine the heat transfer and friction effects. PEC is defined as the ratio of the Nusselt number ratio (with tape to without tape) to the friction factor ratio at the same inlet parameters.

$$PEC = \frac{Nu - Nu_0}{(f - f_0)^{1/3}} \tag{16}$$

The variation of PEC with Reynolds number at different twisted ratio and different shrink ratio is shown in Fig. 15 and Fig. 16. In general observation, the PEC value decreases as the Reynolds number increases, additionally, the twisted ratio at 4 and the shrink ratio at 3.33 provide higher PEC values.
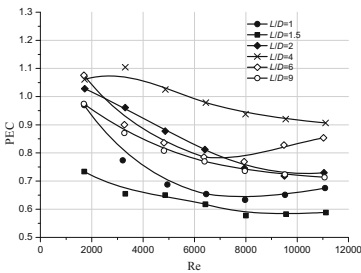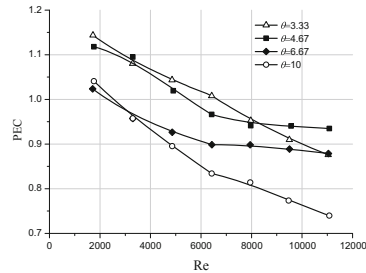

Fig. 15. PEC of twisted tape

Fig. 16. PEC of ripple tape

5   Conclusions

In this paper, the heat transfer enhancement measures of heat exchanger tube are studied by numerically method. By means of inserting different types of tape, the heat transfer intensity can be improved significantly despite the pressure drop will increases correspondingly. For the twisted tape, the intensity of heat transfer enhancement is affected

by twisted ratio, the lower twisted ratio, the higher reinforcement. When the Reynolds number is 10000, the Nusselt number with twisted ratio at 1 is 267% of the Nusselt number without twisted tape. For the ripple tape, the intensity of heat transfer enhancement is affected by shrink ratio, the Nusselt number will increases when the shrink ratio increases. PEC is defined to value the overall performance of the inserts, it shows that in general the twisted tape with twisted ratio at 4 and ripple tape with shrink ratio at 3.33 provide the best performance in consideration of the heat transfer and pressure drop. Base on the results of the CFD, four correlations were developed to predict the heat transfer and flow characteristics of the tube with inserts.

1. References

1. Ray, S., Eder, R., Wittenschlaeger, M., Jaeger, I., Uhlig, V., Trimis, D.: Numerical and Experimental Investigation of Heat Transfer Augmentation Potential of Wire-Loop Structures. J Sci Commun **90**(12), 370–384 (2015)
2. Pawar, S., Sunnapwar, K.: Experimental and CFD Investigation of Convective Heat Transfer in Helically Coiled Tube Heat Exchanger. J Chem Eng Res Des **92**(11), 2294–2312 (2014)
3. Tang, X., Dai, X., Zhu, D.: Numerical Investigation of Convective Heat Transfer and Fluid Flow in Twisted Spiral Tube. J Heat Mass Transfer **90**(10), 523–541 (2015)
4. Gorman, M., Krautbauer, R., Sparrow, M.: Thermal and Fluid Flow First-Principles Numerical Design of an Enhanced Double Pipe Heat Exchanger. J Appl Therm Eng **107**(1), 194–206 (2016)
5. Bergles E. The imperative to enhance heat transfer in Energy Conservation Through Heat Transfer Enhancement of Heat Exchangers. NATO Advanced Study Institute, Izmir, Turkey;1998.
6. Bergles E, Jensen K, Shome B. Bibliography on enhancement of convective heat and mass transfer, RPI Heat Transfer Laboratory Report HTL-23, New York,1995.
7. Balaras, A.: A review of augmentation techniques for heat transfer surfaces in single-phase heat exchangers. J Energy **15**(10), 899–906 (1990)
8. Naphon, P., Nuchjapo, M., Kurujareon, J.: Tube side heat transfer coefficient and friction factor characteristics of horizontal tubes with helical rib. J Energy Conversion and Management **47**(18–19), 3031–3044 (2006)
9. Kalinin, K., Dreytser, A., Zakirov, G.: Improvement of heat transfer in tubular heat transfer exchangers by the use of grooved tubes J Heat Transfer-Soviet Research **13**(4), 30–40 (1981)
10. Sparrow, M., Prata, T.: Numerical solutions for laminar flow and heat transfer in a periodically converging-diverging tube, with experimental confirmation. J Numerical heat transfer **6**(4), 441–461 (1983)
11. Zimparov, V.: Enhancement of heat transfer by a combination of three-star spirally corrugated tubes with a twisted tape J. Int. J. Heat Mass Transf. **44**(2), 551–574 (2001)
12. Zimparov, V.: Enhancement of heat transfer by a combination of a single-star spirally corrugated tubes with a twisted tape. J Experimental Thermal and Fluid Science **25**(4), 535–546 (2002)
13. Zimparov V. Prediction of friction factors and heat transfer coefficients for turbulent flow in corrugated tubes combined with twisted tape inserts. Part 1:friction factors. J International Journal of Heat and Mass Transfer 2004; 47(2): 589–599.
14. Zimparov V. Prediction of friction factors and heat transfer coefficients for turbulent flow in corrugated tubes combined with twisted tape inserts. Part 2: heat transfer coefficients J International Journal of Heat and Mass Transfer 2004;47(1): 385–393.

15. Bas, H., Ozceyhan, V.: Heat Transfer Enhancement in a Tube With Twisted Tape Inserts Placed Separately From the Tube Wall. J Sci Therm. Fluid **41**(1), 51–58 (2012)
16. Savekar A, Jangid D, Gurjar M, Patil V, Sewatkar C. Analysis of Heat Transfer in Pipe With Twisted Tape Inserts. Second International Conference on Fluid Flow Heat and Mass Transfer; 2015 Apr 30–May 1; Ottawa, Canada. 2015. p. 45–57.
17. Savekar A. Investigations on Flow and Heat Transfer Characteristics of a Tube Equipped With Twisted Tape Inserts. IEEE International Conference on Energy Efficient Technologies for Sustainability (ICEETS); 2015 Apr 10–12; Nagercoil, India. 2015. p. 101–107.
18. Salman S, Kadhum A, Takriff M, Mohamad A. Numerical Investigation of Heat Transfer and Friction Factor Characteristics in a Circular Tube Fitted With V-Cut Twisted Tape Inserts. 2013, J Sci World 2013;90(2): 49–56.
19. Hossain, S., Kumar, U., Rahman, K.: The Enhancement of Heat Transfer in a Circular Tube With Insert and Without Insert by Using the Finite Element Method. J Procedia Eng **105**(1), 81–88 (2015)
20. Meng, J., Liang, G., Li, X.: Field Synergy Optimization and Enhanced Heat Transfer by Multi-Longitudinal Vortexes Flow in Tube. J Heat Mass Transfer **48**(16), 3331–3337 (2005)
21. Bhuiya, K., Sayem, M., Islam, T., Chowdhury, U., Shahabuddin, M.: Performance Assessment in a Heat Exchanger Tube Fitted With Double Counter Twisted Tape Inserts. J Heat Mass Transfer **50**(2), 25–33 (2014)
22. Zhang, X., Liu, Z., Liu, W.: Numerical Studies on Heat Transfer and Friction Factor Characteristics of a Tube Fitted With Helical Screw-Tape Without Core-Rod Inserts. J. Heat Mass Transfer **60**(1), 490–498 (2013)
23. Mahfouz A. 2017, "Numerical Investigation of Heat Transfer and Fluid Flow in Heat Exchangers With Inserts," Ph.D. thesis, Cairo University, Giza,Egypt.
24. Eiamsa-ard, S., Thianpong, C., Eiamsa-ard, P.: Turbulent Heat Transfer Enhancement by Counter/Co-Swirling Flow in a Tube Fitted With Twin Twisted Tapes. J Sci Exp Therm Fluid **34**(1), 53–62 (2010)